Technical Note (Data and Metadata)

Support to Microwave Scatterometer Measurements during MOSAiC

Skytek Subcontract No. H2O/20/4500019119

EUMETSAT Purchase Order No. 4500019119

Table of Contents

Abstract

The MOSAiC expedition provided the unique opportunity to acquire a benchmark data set of multi-frequency Ka-, Ku-, X-, C- and L-band in situ microwave scatterometer data. The dataset was collected between October 2019 and October 2020. This technical note summarizes the specifications of the in situ scatterometer systems, together with campaign implementation plan, data preprocessing, and analysis-ready data and metadata. The MOSAiC multi-frequency scatterometer campaign was a success and the processed data is of high quality.

MOSAiC remote sensing team collected the radar data. Data were collected over 5 Legs from various remote sensing sites on the MOSAiC floe, with measurements spanning from sea ice freeze-up and advanced melt thermodynamic regimes. Scatterometer measurements were supported with various meteorological and snow/sea ice geophysical property measurements covering the remote sensing footprint. Overall, the multi-frequency scatterometer datasets are very important to understand and quantify critical snow/sea ice state variables such as snow depth, sea ice thickness, freeze-up and melt-onset timings and characterizing the seasonal evolution of snow-covered sea ice thermodynamics.

1. Multi-Frequency Microwave Scatterometer System

The multi-frequency microwave scatterometers operated at five different frequencies: L-, C-, X-, Ku- and Ka-band. The systems are manufactured by ProSensing Inc. The Ka- and Ku-band radar (KuKa Radar) is owned by the University of Manitoba, Canada (Prof. Julienne Stroeve). The X-band scatterometer (X-Scat) is owned by the University of Waterloo, Canada (Prof. Claude Duguay). The C-band scatterometer (C-Scat) is owned by the University of Calgary, Canada (Prof. John Yackel). The L-band scatterometer (L-Scat) is owned by the University of Victoria, Canada (Dr. Randall Scharien).

1.1 Ka- and Ku-band Radar (KuKa Radar)

The KuKa radar transmits Ka-band waves at 30-40 GHz and Ku-band waves at 12-18 GHz, with bandwidths of 6 and 10 GHz for the Ku- and Ka-bands, respectively (Figure 1). The instrument was designed to operate in both a ‘stare’ and ‘scan’ mode during the MOSAiC expedition. Operating parameters of the KuKa Radar are summarized in Table 1. The radar operated in the permanent ‘scan’ mode while at the different remote sensing sites in during Legs 1, 2, 4 and 5; with an idle time of 30 minutes (Leg 1) and an hour (Legs 2, 4 and 5) between the scans. In the ‘scan’ mode, the radar was programmed to acquire scans along an azimuthal angle range of 90° (between -45° and +45°), at incidence angles between nadir and 50°, at 5° increments (during Legs 1 and 2), and between nadir and 60°, at 3° increments (Legs 4 and 5). In total, 3308 hourly scans were acquired during the year-long campaign.

In the ‘stare’ mode, the KuKa radar was mounted on a smaller sled in a nadir-looking configuration and towed with a snowmobile or by hand along the northern and southern transect loops. During Leg 1, only 2 short transects were done by hand, whereas during Leg 2 with the PI on board, full northern and half of the southern transects were carried out every week from mid-December to end of January in the ‘stare’ mode, using skidoos. During Leg 2 additional sampling on leads, frost-flowered thin ice and first-year ice floes were made. Further, during Leg 2, more detailed sampling and supporting observations were made to support interpretation of the data, and thus the analysis of the data is more robust during this time-period.

Figure 1: The KuKa radar system deployed at MOSAiC in 'scan' (left) and 'stare' (right) modes. (**Photo Credit**: Stefan Hendricks).

Table 1. Summary of KuKa radar specifications.

	Ku-band	**Ka-band**
Radar Parameter	**Value**	**Value**
RF output frequency	12-18 GHz	30-40 GHz
Transmit power	10 dBm	6 dBm
Transmit bandwidth	6 GHz	10 GHz
Range resolution	2.5 cm	1.5 cm
Antenna 6-dB two-way beamwidth	16.9º at 13.575 GHz	11.9º at 35 GHz
Cross-polarization isolation	>30 dB	>30 dB
Transmit/receive polarization	VV, HH, HV, VH	VV, HH, HV, VH
Noise Floor	-70 dB (VV,HH) -80 dB (HV, VH)	-90 dB (VV,HH,HV,VH)

1.2 X-band Scatterometer (X-Scat)

The X-band scatterometer (X-Scat) transmits X-band waves at 9.6 GHz at 0.5 GHz bandwidth (Figure 2). Operating parameters of X-Scat are summarized in Table 2. The radar operated in the permanent mode at the remote sensing site only during Leg 2. The radar was programmed to acquire scans along an azimuthal angle range of 60° (between 0° and +60°), at incidence angles between 21° and 60°, at 3° increments. No observations were acquired during Legs 1, 3, 4 and 5 as the instrument suffered multiple technical damages and had to be retreated from the remote sensing site.

In total, 2 weeks of winter measurements in January 2020 were acquired, collected coincident with other scatterometers. During the initial phase of Leg 2, the X-Scat system had to retreated to the ship on 28 December, since the radar system was working but the tracker was dysfunctional. The tracker was diagnosed, and it was found that the tracker loses its configuration file which led the tracker unable to respond to azimuth and incidence angle movement commands.

The tracker was uploaded with new configuration file and a defective capacitor was replaced which solved the problem. Upon repair and refurbishment, the X-Scat was redeployed on 16 January and started measuring. The scans were done manually from the remote sensing hut and downloaded. No usable X-Scat measurements were recorded in Leg 1.

On 30 January, the X-Scat stopped working. The system was retreated to the ship on 5 February and diagnosed. It was found that the X-Scat computer motherboard installed inside the data acquisition box had failed, due to presence of snow in the circuit, causing it to short circuit the system. Since the X-Scat system did not have any spare computer, it was decided to wait until Leg 4 for the spare parts to be brought in. On 15 February, the X-Scat was packed onto respective boxes.

Figure 2: The X-Scat system deployed at MOSAiC. (**Photo Credit**: Gunnar Spreen).

Table 2. Summary of X-Scat specifications.

	X-band
Radar Parameter	**Value**
RF output frequency	9.65 GHz
Transmit bandwidth	0.5 GHz
Range resolution	30 cm
Antenna 6-dB two-way beamwidth	4.3° at 9.65 GHz
Transmit/receive polarization	VV, HH, HV, VH
Noise Floor	-50 dB (VV, HH, HV)

1.3 C-band Scatterometer (C-Scat)

The C-band scatterometer (C-Scat) transmits C-band waves at 5.52 GHz at 0.5 GHz bandwidth (Figure 3). Operating parameters of C-Scat are summarized in Table 3. The radar operated in the permanent mode at the remote sensing site during Legs 2 and 3. The radar was programmed to acquire scans along an azimuthal angle range of 90° (between 0° and +90°), at incidence angles between 18° and 60°, at 3° increments. No observations were acquired during Legs 1, 4 and 5. In total, 464 scans were acquired during winter and early-melt seasons, collected coincident with other scatterometers.

Since 3 February, the C-Scat operated in a permanent scanning mode stationery at the remote sensing site. The C-Scat is presently programmed to measure manually 5 to 10 scans every day, between 0° to 45° azimuth-, and at 24° to 60° (at 3° steps) incidence-angle range. The C-Scat scan files are automatically copied every night at 0400 hrs (ship time), from the C-Scat ELNORA server to the MOSAiC Central Storage. During Leg 1, although C-Scat measured continuously, it was later found during Leg 2 that the measurements were noise, and that the tracker/positioner lost its configuration file. No usable C-Scat measurements were recorded in Leg 1. Therefore, the C-Scat was retreated to the ship for repair on 28 December.

C-Scat underwent multiple rounds of refurbishments: Replacement of C-Scat tracker/positioner by a spare tracker from the X-Scat system. The C-Scat tracker was replaced after two tracker motor capacitors were found to be defective. Although the capacitors were replaced, we found multiple hardware failures (including motor circuit), which led to a decision to replace the tracker with the spare X-Scat tracker. The replacement was successful. It was also found that, during the diagnosis, the power supply unit installed on the C-Scat RF unit and the oscillator generator circuit was defective. The power supply was replaced with a spare unit obtained from the ship's workshop, while a switch had to be installed to activate the oscillator circuit. Both replacements were successful. Following extensive and successful troubleshooting, repair and refurbishments, C-Scat was redeployed on the RS site on 2 February and started measuring from 3 February. Initial scans after redeployment were sent to the PI and ProSensing for data quality check (successful).

Table 3. Summary of C-Scat specifications.

	C-band
Radar Parameter	**Value**
RF output frequency	5.52 GHz
Transmit bandwidth	0.5 GHz
Range resolution	30 cm
Antenna 6-dB two-way beamwidth	5.4° at 5.52 GHz
Transmit/receive polarization	VV, HH, HV, VH
Noise Floor	-30 dB (VV, HH, HV)

Figure 3: The C-Scat system deployed at MOSAiC. (**Photo Credit**: Gunnar Spreen).

1.4 L-band Scatterometer System (L-Scat)

The L-band scatterometer (L-Scat) transmits L-band waves at 1.26 GHz at 0.5 GHz bandwidth (Figure 4). Operating parameters of C-Scat are summarized in Table 4. The radar operated in the permanent mode at the remote sensing site during Legs 1, 2, 4 and 5 and partially during Leg 3. During Leg 3, the L-Scat was damaged by falling on the ice during a strong storm and could not be repaired and redeployed. The system was repaired in Leg 4 and deployed successfully in Legs 4 and 5. The radar was programmed to acquire scans along an azimuthal angle range of 90° (between 0° and +90°), at incidence angles between 15° and 63°, at 3° increments. In total, 3830 scans were acquired during MOSAiC, coincident with other scatterometer measurements.

Table 4 Summary of L-Scat specifications.

	L-band
Radar Parameter	**Value**
RF output frequency	1.26 GHz
Transmit bandwidth	0.5 GHz
Range resolution	30 cm
Antenna 6-dB two-way beamwidth	14° at 5.52 GHz

Transmit/receive polarization	VV, HH, HV, VH
Noise Floor	-30 dB (VV, HH, HV)

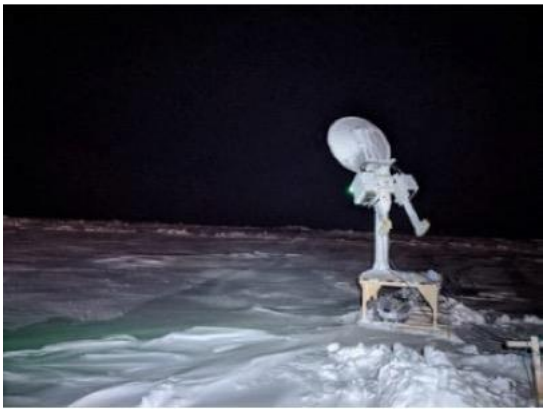

Figure 4: The L-Scat system deployed at MOSAiC. (**Photo Credit**: Vishnu Nandan).

2. Remote Sensing Sites on MOSAiC Floe

The scatterometers were deployed at strategically located remote sensing sites on the MOSAiC Floe inside the Central Observatory in the proximity of RV Polarstern but looking towards an undisturbed “no-walk” zone, where the snow and sea ice will develop undisturbed from other measurements of the campaign. The scatterometers were powered by a central power line from the ship. Flotation was added to keep the instruments afloat in case of emergency and ice break-up. When the ice floe broke up, the instruments were retreated to the ship. All measurements will be taken either quasi-continuously or with at least weekly repetition to fully cover the complete seasonal cycle from winter, spring, to summer.

2.1 Remote Sensing Sites #1 and #2 (Leg 1)

Measurements at Remote Sensing Site (RSS) #1 started on 18 October 2019 with the installation of the KuKa radar. See the tables in the appendix for a list of measurement durations for each instrument. Figure 5 shows the layout of the site on 10 November 2019 with the surface topography from airborne laser scanning in the background. The photos in Figure 6 give an overview of the RSS1 site.

All instruments look at a homogenous ice area with similar properties typical for the southern part of the floe at that time: second year (or remnant) ice with a dominant fraction (>60%) of melted-through melt ponds. The new ice in the melt pond areas have in most cases first-year ice (FYI) properties and will be referred to as FYI here. Typical ice thickness at the beginning of November

for the dominant level ice in the footprints of scatterometers was 60±5 cm. However, some thicker remnant ice could also be present. The thicker ridges/rafted areas, the instruments were deployed on, had a thickness of about 2 m. Snow depth was 10±5 cm for the level ice areas (all measurements from thermistor chain deployments). On 16 November 2019 cracks appeared at the site and parts of the ice got depressed. All measurements stopped and instruments were retreated closer to the remote sensing hut. In the following days more and more cracks appeared, which later partly ridged, and this part of the floe got sheared away about 500 m towards the port side of Polarstern. The former measurement area got first flooded and later destroyed. On 26 November all instruments and the hut were moved to the new RSS #2.

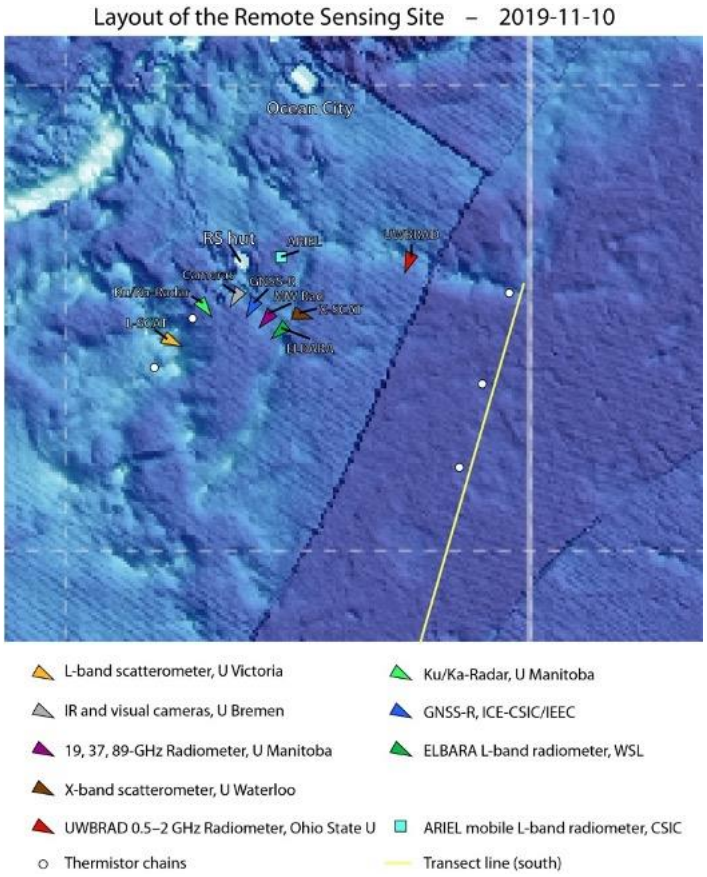

Figure 5: The map shows the status of the Remote Sensing Site 1 on 10 November 2019 with the ALS surface topography map from 20 October 2019 as background.

Figure 6: Remote Sensing Site with scatterometers on 2nd November 2019. The right image shows the same instruments from the opposite point of view. (Photo Courtesy: Stefan Hendricks).

After the relocation of the RS hut and all instruments on 26 November and re-establishing power on 28 November the first measurements at the RSS #2 started on 29 November. The full set of instruments (besides X-SCAT) was operational again on 10 December 2019. Figure 7 shows a map of the site on 12 December 2019 with the ALS surface topography from 6 December in the background, the photo in Figure 8 gives an overview of the site layout.

The ice and snow properties at RSS #2 site are like the ones at RSS #1 site. Because of the vicinity of more ridges the snow depth was slightly higher. The ice thickness of the level ice was 70–80 cm at the beginning of December (from initial drillings and thermistor chain deployments). Snow depth was about 9±5 cm for the level ice. However, increased snowfall and wind in the first week of December caused snow dunes to build up behind some of the instruments. Luckily the south-western wind deposited most of the snow outside the measurement field. Still this event increased snow depth for the snow dune areas while the snow depth on the level ice even slightly (~2 cm) decreased. This results in a mean snow depth of 18±9 cm along the RS instruments on 10 December 2019 (all from ruler stick measurements and thermistor chain deployments).

On Friday the 13 December, the day of the arrival of Kapitan Dranitsyn, again cracks appeared at the remote sensing site. By 14 December all instruments were retreated to the RS hut and measurements stopped. On 15 December the site was handed over to leg 2. By then the cracks started to freeze over and a small ridge build up at one of them. If the situation stayed stable as this Leg 2 personnel planned to continue the measurements at RSS #2.

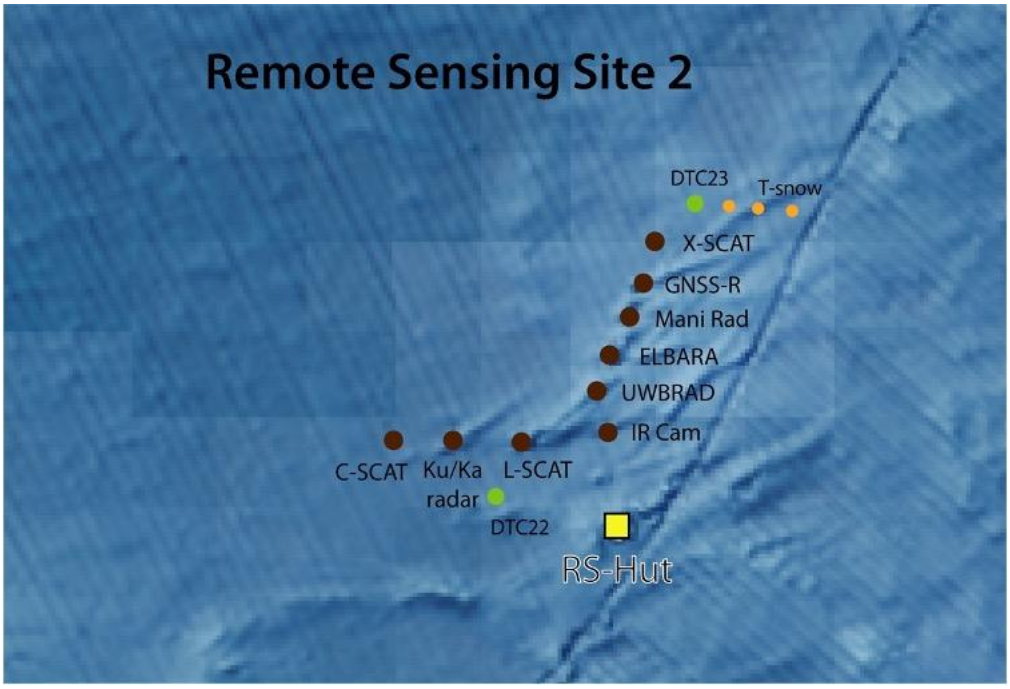

Figure 7: Map with the layout of the RSS #2 on 12 December 2019 with the ALS topography map from 6 December 2019 in the background.

Figure 8: Overview of the RSS #2 on 8 December 2019. From left to right: X-SCAT, GNSS-R, 19-37-89 GHz radiometer, IR/web cameras (in back), ELBARA, UWBRAD, L-SCAT, Ku/Ka radar, C-SCAT (Photo: Stefan Hendricks)

2.2 Remote Sensing Sites #3 (Leg 2)

When Leg 2 arrived, none of the on-ice remote sensing instruments were measuring. This is because they were threatened by large cracks on three sides of RSS #2 and were moved closer to the hut. The Leg 2 remote sensing team started to redeploy the instruments on 21 December nearby the old site. By the end of December, the team had KuKa radar and L-Scat operational. The RSS #3 was maintained throughout Leg 2 and successfully handed over to the Leg 3 remote sensing team.

After Leg 1 left, Leg 2 evaluated the stability and feasibility of the site, and it was determined the instruments would be redeployed a bit further east of the previous site. The RSS #3 was established on 21 December, and setup in an ‘L-shaped’ geometry near the old RSS #2 site sharing about 60% of the previous RSS #2 area. This site primarily consisted of a refrozen melt pond on second year ice. The first instrument redeployed was the KuKa radar and it collected data starting at 19:30 UTC. However, since the new RSS #3 site was located a bit further form the hut than the RSS #2 site, we decided to move the hut closer to the instruments on 30 December. This required power to be turned off to the instruments for a short period of time.

As of 23 February 2020 and 03 March 2020 (Return from Polarstern to Dranitsyn), C-Scat and L-Scat were operational and measuring. Figure 9 shows the site layout as of 19 February, acquired from the visual camera (from the University of Bremen), installed on the top of the RS hut.

Figure 9: Overview of RSS #3 site as of 19 Feb 2020. (Photo: Screenshot from the University of Bremen's visual camera, installed on top of the RS hut).

The ice and snow properties at RSS #3 site are similar to that of RSS #1 and RSS #2 sites (refrozen melt-ponded second-year sea ice). Regular snow depth measurements were taken directly in front of every instrument (without disturbing the scan area), using an avalanche snow depth probe and recorded. With frequent blowing snow and accumulation events, snow depths increased from ~ 10 cm (measured on 23 Dec) to a maximum of ~ 81 cm (measured on 22 Feb) (Figure 10). The ice thickness was ~90 cm during the beginning of Leg 2, which further increased to 121 cm by 15 Jan (from ice core drillings). Occasional salinity ice cores were also taken behind the instruments, with the top 15 cm were almost found to be brackish (0.8±0.2 psu), and higher salinities towards the bottom (5.2±1.2 psu).

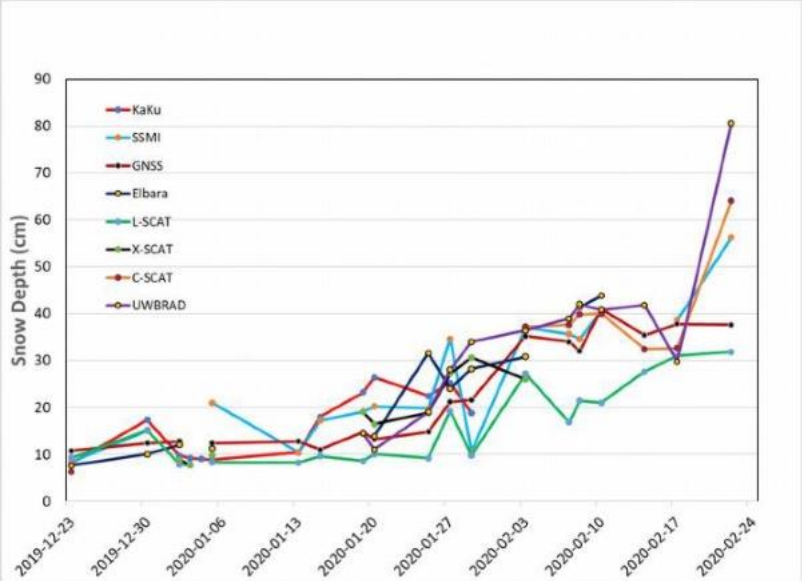

Figure 10: Snow depth measurements recorded during Leg 2, around the instruments in the RSS #3 site.

2.3 Remote Sensing Sites #4 (Leg 3)

When Leg 3 arrived, the RSS #3 was functional, and measurements were ongoing with C-Scat and L-Scat. The RSS #3 was established and brought to operational status during Leg 2. The measurements were ongoing at this site until 11 March 2020 when a crack opened up at the site cutting the site away from the main floe. This crack passed by close vicinity of the RS hut as well as few other RS instruments. On the evening of 11 March, a team of four personnel from the ICE team and the logistics were dropped on site by helicopter to move the instruments away from the lead to save them from possibly drowning and/or being crushed by the anticipated ridge formation. Figure 11 show a picture of RSS #3 after the crack in the ice and the RS hut conditions after ridge formation at RSS #3, respectively.

Figure 11: (a) Overview of RSS #3 site on 11 March 2020; (b) RS hut on 17 March 2020 endangered by the forming ice ridge. (photos: (a) by Reza Naderpour, panel (b) by Lars Kaleschke).

Therefore, on 11 March 2020, all measurements on RSS #3 had to be stopped. After the ridge formation and increased danger of serious damage to the RS hut and instruments, the decision to was made relocate the site. Therefore, given the highly dynamic ice conditions on the floe hosting RSS #3 and the Met City, the instruments were brought to the logistic area to be redeployed at RSS #4.

The RS team decided to situate the RSS #4 closer to the ship. Given the strong ice dynamics and the shrinking size of the stable parts of the floe, this decision made sense because a) it was situated on a fairly stable part of the floe, b) it would provide easy access to the site without necessary bear guarding and even in sub-optimal weather conditions, and c) it would make it exponentially easier to save the instruments given the short distance to the logistic area and reach of the ship's cranes. Figure 12 shows the location of instruments on a TLS snow map. RSS #4's operation continued until the planned end date of scientific measurements on Leg 3 on the ice after which the instruments were packed and brought onboard Polarstern.

2.4 Remote Sensing Sites #5 (Leg 4)

Leg 4 was a fresh start for the remote sensing program since no instrument or infrastructure was left on the floe at the end of Leg 3. The major task for the Leg 4 remote sensing team was to find and establish a new site for the remote sensing program. In addition, a substantial amount of time was spent on repairing and troubleshooting broken instruments from previous legs. Setting up and maintaining the main site was challenging given the melting conditions at the floe.

The first remote sensing measurements were recorded on June 26, 2020, and lasted until July 30, 2020, a day before the floe broke up. During Leg 4, the RS team acquired time series and discrete measurements from KuKa radar and L-Scat. These measurements were accompanied by regular snow pits and ice core measurements. In addition to calibrating L-Scat, the team also performed destructive experiments at the site towards the end of the measurement cycle.

Determining the location of RSS #5 was exceptionally challenging. Based on the search criteria (e.g., stability, quick infrastructure development, etc.), the RS team had to limit ourselves to second-year ice. Their goal was to find a stable location at close proximity to the ship so that power and network connections could be established in the earliest phase of the new infrastructure development on the floe.

After scouting the floe areas, finally, the team found a suitable location for the RSS #5, which was approximately 100 m away from the ship. This site was surrounded by small ridges, which offered a gentle slope to the center of the scanning area. The floe had thicker snow on the site, perhaps deeper than any previous sites during MOSAiC. The first snow sampling at the site recorded 70 cm of an isothermal snowpack. Meltwater at the snow-ice interface was also found. The evolution of the RSS #5 can be seen from Figures 12-14.

Figure 12: RSS #5 on the MOSAiC (fortress) floe during Leg 4. The picture was taken during the early operational phase on July 01, 2020. Photo: Aikaterini Tavri.

Figure 13: Operational RSS #5 on July 14, 2020. Photo: On-site camera.

Figure 14: RSS #5 surrounded by melt ponds on July 29, 2020, two days prior to floe break-up. Airborne Photo: Jonathan Hamilton.

2.5 Remote Sensing Sites #6 (Leg 5)

The RSS #6 site was operational from 22nd August, one day after the arrival, until 19th September, the last day before leaving the floe. The site was established about 200 m away from the ship at a central position in the CO. The site remained stable throughout Leg 5. Figure 15 shows a map with the layout of the RSS #6 site with an aerial picture from 6th September in the background. The site has homogenous ice in the centre and is framed by melt ponds on three sides. The photos in Figure 16 give an overview of the RSS #6 site.

All instruments look at a homogenous ice area with similar properties. The initial ice thickness on 22-24 August was 137±2 cm and did not change significantly until the end (19 September ice thickness: 136±2 cm). At the beginning there was a surface scattering layer of about 2 to 5 cm depth. At the end snow depth was 4±0.5 cm.

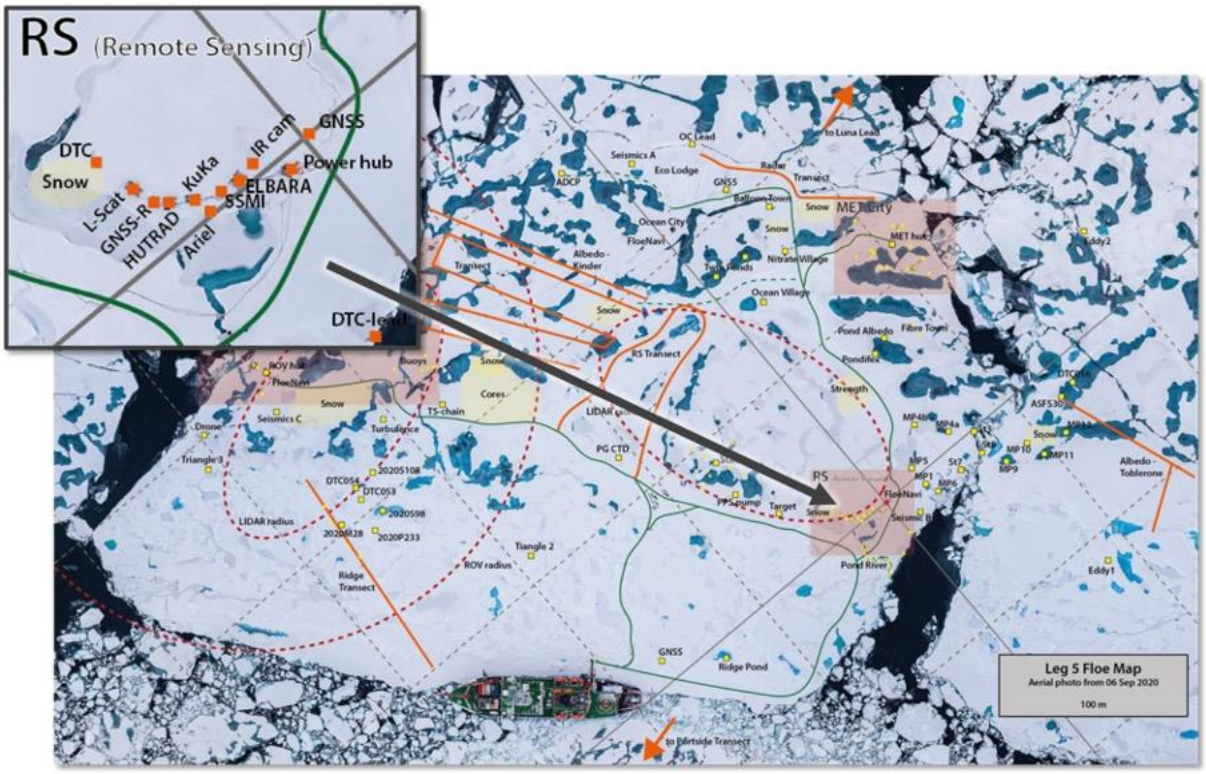

Figure 15: Map of the Lg 5 Central Observatory. The detail on the top left shows the RSS #6 site layout. The background shows an aerial photo (Courtesy: Steffen Graupner/Charles Finkbeiner) taken by a drone on 6 September 2020.

Figure 16: RSS #5 on 29 August (left image) and 8 September 2020, when all instruments were deployed. The homogenous ice area seen in the front of the right image was the main target area for the RS measurements. (Photos: Gunnar Spreen)

The KuKa radar was operated along a short about 150 m long “radar transect” on a regular basis to account for spatial variability. As the frame for the transect sled was sent back after Leg 3 by accident, the RS team towed the radar along the transect in nadir configuration on its original sled. The L-Scat fell over during Leg 3 and needed some repair during Leg 4. As a consequence, the scanning mechanism was not working smoothly all the time and the scans sometimes had a wobbly or wavy motion. This effect was worth at higher elevations, which therefore were avoided during later scans.

3. Scatterometer Data Processing

3.1 KuKa Radar

Detailed description of radar specifications, signal processing, polarimetric calibration routine, and error determination for both ‘scan’ and ‘stare’ modes can be found in Stroeve et al. (2020). KuKa radar acquires VV, HH, HV and VH fully-polarimetric data. In addition, a calibration loop signal and a noise signal are recorded. Thus, for each block of data collected, six signals are processed. Data are processed into range profiles of the complex received voltage, through fast Fourier transform (FFT). The range profiles for each polarization combination are power-averaged in azimuth for each incidence angle.

In ‘stare’ mode, the range profiles can be spatially averaged to reduce variance, done similarly in Stroeve et al. (2020). However, in this report we have also processed each individual radar returns. Similarly, for the scan mode, the entire azimuthal range is averaged, or in different azimuthal bins for every incidence angle.

The linear FM signal for each polarization state has a duration of 2 ms, followed by a 100 ns gap. Thus, the total time required to gather the data used in computing the complex received voltages is 8.3 ms. To assure proper estimation of the co-polarized correlation coefficient and phase difference, it is important that the antenna moves much less than half an antenna diameter during the time period between the VV and HH measurements (2.1 ms). Using an allowable movement of 1/20 of antenna diameter in 2.1 ms, the maximum speed of the sled during the nadir measurements is limited to approximately 2.1 m/s at Ka-band and 3.5 m/s at Ku-band. The software provided by ProSensing converts the Ku- and Ka-band raw data in both stare and scan modes, into calibrated polarimetric backscatter and parameters of the target covariance matrix and/or Mueller matrix. This has been updated into a new python package KuKaPy, a faster and open-source package to process KuKa data. The package is translated from the original licensed IDL. KuKaPy will be made available to public via GitHub and will allow users to conduct open-source based analysis on KuKa data. Testing of the output shows high accuracy between KuKaPy- and IDL- derived KuKa output.

The Ku- and Ka-band signal processing, calibration procedure, derivation of polarimetric backscatter and parameters, and system error analysis are implemented similar to the C- and X-band scatterometer processing, built and implemented by ProSensing, and described in detail by Geldsetzer et al. (2007) and King et al. (2013), respectively.

3.2 X-, C- and L-band Scatterometer Data Acquisition

During data acquisition, the X-, C- and L-band scatterometer systems acquire data on a series of six signal states: the four transmit polarization combinations (VV, HH, HV and VH), a calibration loop signal and a noise signal (similar to KuKa radar). Each data block consists of these six signals and are processed separately for each frequency. Data are processed into range profiles of the complex received voltage, via Fast Fourier Transform (FFT). The range profiles for each polarization combination are power-averaged in azimuth for each elevation angle. The scatterometer scans within a programmed elevation angle range, moving from low to high at prescribed increments. For each elevation angle, it moves across a prescribed azimuthal angular width. A new file is generated each time the positioner begins a scan. The scan area during one complete scan is a function of the elevation range, the azimuth range, the antenna beamwidth, and the system geometry, with the instantaneous beam footprint increasing in area, as elevation angle increases.

3.3 Scatterometer Data Formats

The raw data are stored in the scatterometer system as .dat files and need to be manually downloaded from the radar's internal data drive. An IDL program (for X-, C- and L-scats) is used to process the raw files and convert them into readable output data. The same is done by the KuKaPy python package for KuKa radar data. The KuKaPy package is a translated version of the IDL package initially built for all scatterometer systems. The IDL and python code ingests the raw

data using a calibration file, to generate a complex scattering matrix, a second-order covariance matrix, fully-polarimetric backscatter (VV, HH, HV and VH; in dB scale), and polarimetric parameters such as the co-polarized phase difference (in degrees) and the co-polarized correlation coefficient. For KuKa radar data, the KuKaPy package also extracts range power echoes for every radar 'shot' and individual backscatter for radar detected geophysical interfaces (e.g. air/snow, internal snow, snow/ice). This backscatter calculation procedure is performed on the average of all data blocks within the azimuthal angular width, for each incidence angle. Using the polarimetric backscatter, a user can derive other parameters such as the co-polarized and cross-polarized ratios, co-polarized phase difference, co-polarized correlation coefficient, total power etc. In every step of IDL/python processing, a user will be able to see the power-range and polarization signature plots for every incidence angle step; these can be individually saved by modifying the IDL/Python script. The user can also modify the configuration .txt files to change the processing routine.

The final processed files from all scatterometer systems contain the date and time information (UTC), range peak signal, Mueller, covariance matrix, total backscatter, co-polarized phase difference and co-polarized correlation coefficient for all incidence angles. The KuKa radar and L-Scat data also have positional information (latitude and longitude) as recorded by the onboard GPS.

The final processed files from the KuKa radar are exported as netcdf files, while the X-, C- and L-band scatterometers are saved as .nrcs files that contain can be imported into any text reading program for data analysis. In the near future, once the X-, C- and L-band scatterometer IDL scripts are translated into python packages, netcdf formatting of processed files will be implemented similar to that of KuKa radar.

4. Data and Metadata Availability

All final data and metadata of all scatterometer measurements will be stored at the MOSAiC Central Storage (MCS) and at PANGAEA (World Data Center PANGAEA Data Publisher for Earth & Environmental Science (www.pangaea.de) after post-processing and quality checks. Storage and release of data follow the MOSAiC data policy. All data and metadata are handled, documented, archived and published following the MOSAiC data policy. Scatterometer instrument PI permission is required to access, analyse and publish data before 1st January 2023. Data will be freely and publicly available on 1st Jan 2023 abiding by MOSAiC Data Policy. From this date, there are no restrictions on data usage. However, users are encouraged to communicate with the PI, during access, analyses, interpretation and publishing of data. The status of individual scatterometer data processing is as follows:

- All Ka- and Ku-band (KuKa radar) data have been processed and quality controlled. The raw and processed data in netcdf format are stored in the UK's NERC repository (https://doi.org/10.5285/5fb5fbde-7797-44fa-afa6-4553b122fdef).

- All C- and X-band (C-Scat and X-Scat) data have been processed and quality controlled. Since no external calibration was conducted for these instruments during MOSAiC, data processing is carried out using an internal calibration routine proposed and tested by the instrument manufacturer ProSensing Inc. Additional external calibration files from the instruments conducted from previous field campaigns are available for data quality comparison. Once data processing is complete (expected by mid-December 2022), the raw and processed data (in .txt format) will be made available in a EUMETSAT server.

- The L-band (L-Scat) data is presently undergoing data pre-processing quality checks by the instrument manufacturer ProSensing Inc. and the instrument PI. The quality checks include investigating data from October 2019 to March 2020 at higher incidence angles where L-Scat underwent wind-induced movement of the system during data acquisition. In March 2020, the instrument suffered a major technical failure that was refurbished in July 2020. Data collected after refurbishment is undergoing tests for signal quality (e.g. noise levels, shift in range power at select incidence angles, etc.). Once quality checks and data processing are complete (date to be confirmed), the raw and processed data (in .txt format) will be made available on a EUMETSAT data server.

5. References

Geldsetzer, T., J.B. Mead, J.J. Yackel, R.K. Scharien, and S.E. Howell, 2007. Surface-based polarimetric C-band scatterometer for field measurements of sea ice. *IEEE Transactions on Geoscience and Remote Sensing*, 45(11), 3405-3416.

King, J.M.L., R. Kelly, A. Kasurak, C. Duguay, G. Gunn, and J.B. Mead, 2013. UW-Scat - ground-based dual frequency scatterometry for observation of snow processes. *IEEE Geoscience and Remote Sensing Letters*, 10(3): 528-532, doi: 10.1109/LGRS.2012.2212177.

Stroeve, J., V. Nandan, R. Willatt, R. Tonboe, S. Hendricks, R. Ricker, J. Mead, R. Mallett, M. Huntemann, P. Itkin, M. Schneebeli, D. Krampe, G. Spreen, J. Wilkinson, I. Matero, M. Hoppmann, and M. Tsamados, 2020. Surface-based Ku-and Ka-band polarimetric radar for sea ice studies. *The Cryosphere*, 14(12), 4405-4426, https://doi.org/10.5194/tc-14-4405-2020.